Atmospheric
Measurement
Techniques

Open Access

Improved retrieval of nitrogen dioxide (NO₂) column densities by means of MKIV Brewer spectrophotometers

H. Diémoz[1,2], A. M. Siani[2], A. Redondas[3], V. Savastiouk[4], C. T. McElroy[5], M. Navarro-Comas[6], and F. Hase[7]

[1]ARPA Valle d'Aosta, Saint-Christophe, Italy
[2]Department of Physics, Sapienza – University of Rome, Rome, Italy
[3]Izaña Atmospheric Research Center, AEMET, Tenerife, Canary Islands, Spain
[4]Full Spectrum Science Inc., Toronto, Ontario, Canada
[5]Department of Earth & Space Science and Engineering, York University, Toronto, Ontario, Canada
[6]Área de Investigación e Instrumentación Atmosférica, INTA, Torrejón de Ardoz, Spain
[7]Institute for Meteorology and Climate Research, IMK-ASF, Karlsruhe Institute of Technology (KIT), Karlsruhe, Germany

Correspondence to: H. Diémoz (h.diemoz@arpa.vda.it)

Abstract. A new algorithm to retrieve nitrogen dioxide (NO₂) column densities using MKIV ("Mark IV") Brewer spectrophotometers is described. The method includes several improvements, such as a more recent spectroscopic data set, the reduction of measurement noise, interference by other atmospheric species and instrumental settings, and a better determination of the zenith sky air mass factor. The technique was tested during an ad hoc calibration campaign at the high-altitude site of Izaña (Tenerife, Spain) and the results of the direct sun and zenith sky geometries were compared to those obtained by two reference instruments from the Network for the Detection of Atmospheric Composition Change (NDACC): a Fourier Transform Infrared Radiometer (FTIR) and an advanced visible spectrograph (RASAS-II) based on the differential optical absorption spectrometry (DOAS) technique. To determine the extraterrestrial constant, an easily implementable extension of the standard Langley technique for very clean sites without tropospheric NO₂ was developed which takes into account the daytime linear drift of stratospheric nitrogen dioxide due to photochemistry. The measurement uncertainty was thoroughly determined by using a Monte Carlo technique. Poisson noise and wavelength misalignments were found to be the most influential contributors to the overall uncertainty, and possible solutions are proposed for future improvements. The new algorithm is backward-compatible, thus allowing for the reprocessing of historical data sets.

1 Introduction

Nitrogen dioxide (NO₂) is a key component of the Earth's atmosphere. Despite its low concentration, it drives several chemical reactions leading to both destruction and preservation of ozone (O₃) in the stratosphere (Hampson, 1964; Crutzen, 1970; Jones et al., 1989) and photochemical smog in the troposphere (Haagen-Smit, 1952). Furthermore, NO₂ absorbs solar radiation, thus impacting the radiative balance of the planet (Solomon et al., 1999) and interfering with sun photometric measurements, such as the aerosol optical depth (Shaw, 1976).

In 1985, an automated Brewer ozone spectrophotometer was modified to add capability to measure solar visible radiation and retrieve atmospheric nitrogen dioxide (Kerr, 1989), based on the differential optical absorption technique (Brewer and McElroy, 1973). Nowadays, the Brewer network consists of about 195 instruments installed in 44 different countries throughout the world (Kumharn et al., 2012). Among them, according to the metadata archive of the World Ozone and Ultraviolet radiation Data Center (WOUDC, http://woudc.org/data/MetaQuery/metaquery_e.cfm), more than 60 MKIV Brewer spectrophotometers have been put in operation and long-term nitrogen dioxide records have been collected at the respective stations. Unfortunately, the original algorithm has never been officially updated and exhibits several limitations that prevent users from confidently

employing the measured data for accurate analyses. Remarkable overestimations, up to 100 %, by the Brewer were detected in a wide range of intercomparison campaigns (McElroy et al., 1994; Barton, 2007) along with random deviations as large as 30 % (Hofmann et al., 1995). Even comparisons between MKIV Brewers and satellite radiometers generally show similar issues (Francesconi et al., 2004).

Notable efforts have been done in the last few years to improve the NO$_2$ retrieval by the Brewer, both in the UV-A band with direct sun measurements (Cede et al., 2006) and in the visible wavelength range by collecting the diffuse light from the zenith (Barton, 2007). Nevertheless, high-quality estimates of nitrogen dioxide by the Brewer are still difficult to acquire, mainly owing to the measurement noise drowning out the weak NO$_2$ signal, the effects of instrumental inaccuracies, such as slight wavelength misalignments, and the influence of the atmospheric species absorbing in the same wavelength range (e.g. the oxygen dimer, O$_2$−O$_2$, and water vapour, H$_2$O, in the visible). Finally, no on-site service with reference travelling standards (as available for ozone calibrations) exists to track the NO$_2$ radiometric and wavelength calibration of the Brewer instruments operating worldwide.

A previous study (Diémoz et al., 2013) proved the feasibility of an updated method for retrieving nitrogen dioxide with MKIV Brewers. The present work describes the first application of this algorithm to real data and its validation during an ad hoc field campaign at a high-altitude site. The results will help not only to henceforth collect high-accuracy data series, but also to reprocess with higher accuracy the long-term raw data sets recorded at the existing measuring stations.

2 Measurement site and instruments

The measurements discussed in the present paper were performed at the Izaña Atmospheric Research Center, Tenerife, Canary Islands (28.31° N, 16.50° W, 2400 m a.s.l.) during an ad hoc field measurement campaign in September and October 2012. The site, which is described in more detail by Gil et al. (2008), was chosen to achieve the maximum atmospheric stability necessary for an accurate calibration. On that occasion, Brewer #066 was temporarily moved to the Izaña observatory from its original location, Aosta, Italy, where it has been regularly operating since 2007 (Diémoz et al., 2007). Co-located instruments, associated with the Network for the Detection of Atmospheric Composition Change (NDACC), were used as references for comparison purposes and are thus described below along with the Brewer.

2.1 MKIV Brewer spectrophotometer

The MKIV Brewer spectrophotometer (Kipp and Zonen, 2007) collects solar light reaching the ground from either the sun or the sky. One of the two observation geometries is selected through the use of a reflective prism (to set the elevation angle of the field of view) and a solar tracker (adjusting the azimuth angle). Zenith sky measurements can be performed at two perpendicular, linear polarisations, depending on the tracker position, in a parallel or perpendicular direction to the scattering plane. The light is then dispersed into its spectrum by a holographic plane diffraction grating, rotated by a high-precision stepper motor and operated in the second order. A rotating slit mask at the exit of the monochromator allows the nearly simultaneous measurement of the intensity of the beam at up to six different wavelengths, whose spacing is defined by the distances between the six apertures and the wavelength dispersion at the focal plane. When measuring NO$_2$, the default grating position is normally chosen so that the wavelengths are between about 426 and 453 nm, a spectral range with strong differential structures and close to the maximum absorption by NO$_2$. However, the grating can be rotated to span a full spectral range of about 420–500 nm. The resolution usually ranges from 0.6 to 0.9 nm full width at half maximum (FWHM), depending on the slit and the Brewer type. A photomultiplier tube (PMT) is employed to analyse the intensity of the beam emerging from the monochromator and is maintained in its linearity regime with the help of a set of neutral density filters installed in the fore-optics.

One MKIV Brewer (serial number #066) was thoroughly characterised in the visible range. Several spectral lines from three discharge lamps (Hg, Cd, and Ne) were scanned to assess the instrumental resolution and the wavelength dispersion. The latter was then parameterised with an accurate fitting function (Gröbner et al., 1998). Additionally, the spectral transmission of each neutral density filter was determined using the standard lamp installed inside the instrument.

2.2 Fourier Transform Infrared Spectrometer

Since January 2005, a Bruker IFS 125 HR Fourier Transform Infrared Spectrometer (FTIR) owned by the Institute for Meteorology and Climate Research (IMK) has been measuring at the Izaña observatory. The FTIR is operated in solar absorption geometry. The maximum optical path difference achievable is 250 cm, corresponding to a spectral resolution of 0.0035 cm^{-1}. Normally, a resolution of 0.005 cm^{-1} is applied. The spectrometer is equipped with two photovoltaic semiconductor detectors (InSb and HgCdTe). The spectral range covered is 650 to 5000 cm^{-1} and the NDACC optical filter set is used. The measurement precision is estimated to be within 2 % for most species. More details are provided by Schneider et al. (2005).

2.3 UV-visible spectrometer

A new Multi Axis Differential Optical Absorption Spectroscopy (MAX-DOAS) spectrometer (Remote Absorption Spectroscopy for Atmospheric Species, RASAS-II) has been operating by the Instituto Nacional de Technica Aerospacial

(INTA) since 2011. The instrument collects scattered radiation from the sky in the 415–530 nm spectral range. It is based on a Shamrok SR-163i spectrograph and a 1024×255 pixel DU420A-BU Andor Idus CCD camera. Light enters the spectrograph through a fused silica round-to-line fibre bundle. The fibre end width is 100 μm. The diffraction grating is holographic with 1200 grooves mm^{-1} and blazed at 300 nm. The linear dispersion is 0.11 nm pixel^{-1}. The FWHM of the spectrograph in the selected spectral window ranges between 0.52 and 0.58 nm. The spectrograph and detector are housed in a thermostated hermetic container keeping the spectrograph at a constant temperature, thus maintaining the alignment of the spectra with time.

The RASAS-II instrument uses the differential optical absorption spectrometry (DOAS) technique and air mass factors from radiative transfer code to retrieve the NO$_2$ column. Whereas the instrument automatically takes spectra from 45° solar zenith angle (SZA) to twilight, measurements at low SZAs are considered of poor quality since the accuracy is strongly dependent on the signal to noise ratio and on the atmospheric conditions (aerosol optical depth). Only in extremely clear and stable conditions can the data at low SZAs be used. On the contrary, under these favourable weather conditions, at twilight the technique is reliable and the errors are low. A detailed description of RASAS-II can be found in Puentedura et al. (2012).

3 Algorithm

This section summarises the updated NO$_2$ retrieval method described in more detail by Diémoz et al. (2013). As in the standard Brewer algorithm (Kerr, 1989), the Bouguer–Lambert–Beer formula (Bouguer, 1729) is applied to the solar irradiances I_i measured at several wavelengths λ_i, and the logarithms of the irradiances are linearly combined to remove the interference of other species different from nitrogen dioxide, i.e.

$$\sum_i \gamma_i \log I_i = \sum_i \gamma_i \log I_{0i} - \mu_{\text{NO}_2} X_{\text{NO}_2} \sum_i \gamma_i \sigma_{\text{NO}_2 i} \qquad (1)$$
$$- \sum_j \mu_j \sum_i \gamma_i \tau_{ji}.$$

I_{0i} denotes the flux that would be measured outside the Earth's atmosphere through the ith slit and represents a calibration constant typical of each instrument; μ indicates the air mass factor (AMF) of the different species; X_{NO_2} is the vertical column density (VCD) of nitrogen dioxide, the quantity to be determined by the retrieval procedure; the absorption cross sections of nitrogen dioxide at wavelength λ_i are expressed by $\sigma_{\text{NO}_2 i}$; the j subscript identifies the atmospheric species different from NO$_2$; finally, τ_{ji} is the optical depth of the jth species at wavelength λ_i. If the weighting coefficients γ_i are properly chosen, the last sum is minimised and X_{NO_2} can be determined provided that the extraterrestrial

constant (ETC) of the instrument (first term on the right-hand side) is known.

Compared to the standard algorithm, the new method brings several improvements, which are further described and quantified below:

1. While the former makes use of a subset of all recorded data, i.e. the spectral irradiances at only five wavelengths, and minimises the influence of the Rayleigh scattering, ozone absorption, aerosol extinction (assuming that the aerosol optical depth is approximately linear with wavelength in the measurement range), and spectrally flat factors, the new algorithm includes the measurements that are routinely performed (and saved by every Brewer in the data files) through all six slits. The additional degree of freedom, compared to the standard algorithm, is used to find a combination of the coefficients γ_i that maximise the sensitivity to NO$_2$ and minimise the measurement noise.

   Although this first optimisation has little effect on measurement noise when the grating position is already optimally chosen (cf. point 3), the use of six slits instead of only five interestingly turns out to be beneficial in reducing the Brewer sensitivity to slight wavelength shifts (reduction of about 30 %, for Brewer #066) and to the Ring effect (Grainger and Ring, 1962) (about −80 %, calculated on unpolarised irradiances), which impacts diffuse light during zenith sky measurements. This occurs because the influence of the irradiance registered through the second slit, corresponding to a wavelength of about 431.6 nm, very close to a deep Fraunhofer line, is reduced. A different use of the additional degree of freedom is proposed in Sect. 7.1.

2. The spectroscopic data set employed in the algorithm to calculate the weighting coefficients and the differential absorption cross section was updated to more recent laboratory results (Table 1) according to the recommendations by the NDACC (Van Roozendael and Hendrick, 2012). Furthermore, since I_i is actually the convolution between the solar irradiance spectrum and the instrumental bandwidth at each slit, the cross sections have been downscaled to the Brewer resolution by adopting the formula of Aliwell et al. (2002):

$$\sigma_{\text{corrected}}(\lambda') = \qquad (2)$$
$$- \frac{1}{X} \log \left\{ \frac{\int I_0(\lambda) \exp[-\sigma(\lambda) X] W(\lambda' - \lambda) d\lambda}{\int I_0(\lambda) W(\lambda' - \lambda) d\lambda} \right\},$$

where X is an a priori value of the absorber VCD (a value of 0.1 DU for NO$_2$, typical of stratospheric columns at the measurement site (Brühl and Crutzen, 1993; Gil et al., 2008; Herman et al., 2009) was used in this work), σ the laboratory cross section, and W the slit function. This approach mitigates the so-called "I0

Table 1. Spectroscopic data sets used in the standard and new algorithms.

| Species	Standard algorithm	New algorithm
Rayleigh	same as for O$_3$ retrieval	Bodhaine et al. (1999)
NO$_2$	Johnston and Graham (1976), 298 K	Vandaele et al. (2002), 220 K
O$_3$	Vigroux (1952), 291 K	Bogumil et al. (2003), 223 K
O$_2$–O$_2$	not considered	Hermans et al. (2003)
H$_2$O	not considered	Rothman et al. (2009)

effect" since in actual measurements the spectra – and not their logarithm – are filtered by the slit function.

The update of the cross-section data sets represents a major improvement in the algorithm. Indeed, from previous modelling results (Diémoz et al., 2013) the retrieval using the weighting coefficients and the differential cross-section by Kerr (1989) leads to large overestimations of even more than 50 %. On the other hand, the I0 effect is generally expected to be negligible for NO$_2$ retrievals, since nitrogen dioxide is a weak absorber, unless very large slant column densities are to be measured.

3. An optimal position of the grating, i.e. an optimal set of measuring wavelengths, was found that further reduces the measurement noise and minimises the interference on the retrieval by the oxygen dimer, water vapour, the Ring effect (only affecting zenith sky measurements), the NO$_2$ effective temperature in the atmosphere, and slight instrumental wavelength misalignments. This is required accurately simulating all the previous factors as a function of the grating position by perturbing the Brewer equation (Eq. 1). The final set of wavelengths and weighting coefficients (γ_i) for Brewer #066 are presented in Table 2 together with the standard coefficients by Kerr (1989). The resulting grating position depends on both the spectral dispersion and resolution of a specific instrument.

For Brewer #066, the selected position (micro-step 1012) is close to the default position (1000, corresponding to a shift of about 0.13 nm). This optimisation minimises the interference by water vapour (0.009 DU VCD for a saturated atmosphere, compared to 0.02 DU at the standard position) while keeping almost unaltered the sensitivity to other variables. However, the advantages of a different grating position could be much more evident on other instruments with different dispersion properties. Several European MKIV Brewers were examined and some of them show a wavelength sensitivity as large as −0.20 DU per micro-step at the standard grating position (more than double compared to Brewer #066). For those instruments, the choice of a different wavelength set is likely to substantially improve the Brewer stability.

4. The residual interference by the oxygen dimer has been corrected through the use of the SCIATRAN radiative transfer model (Rozanov et al., 2014) taking into account the atmospheric pressure at the measurement site in case of clear sky and using the standard aerosol profile by Anderson et al. (1986), whereas the influence of O$_2$–O$_2$ is totally neglected in the standard algorithm. The contribution of the O$_2$–O$_2$ correction is usually of the order of 0.02 DU on VCDs for Izaña.

5. Since the spectral transmission of the "neutral" density filters is actually not constant and generally varies, as a function of wavelength, with a different pattern compared to any other factor taken into account in the algorithm, the linear combination is not able to remove this effect. Therefore, a correction factor which depends on the selected filter must be added to the linear combination to compensate the filter interference. As shown by Diémoz et al. (2013), systematic errors as large as 0.2 DU (for Brewer #066 when the thickest filters are used and even larger for different Brewers) may be introduced in the retrieved VCDs if the filter correction is neglected.

6. The air mass factors for zenith sky measurements were calculated in both polarisations at 430 nm with the help of the SCIATRAN full-spherical vector radiative transfer model using the finite difference method (Rozanov and Rozanov, 2010). Vertical profiles obtained from a 2-D chemo-dynamical model (Brühl and Crutzen, 1993) were employed for the purpose. The resulting polarised AMFs differ only by a few percent at SZA = 90° from the NDACC recommended AMFs for Izaña (Van Roozendael and Hendrick, 2012), i.e. 2 and −3 % for the parallel and perpendicular observation geometries, respectively (Fig. 1). Differences become larger (e.g. 30 % at SZA = 95°) when zenith angles beyond 90° are considered and are due to the use of both different atmospheric profiles and radiative transfer models (the polarised AMFs were obtained by a full-spherical solver, the NDACC AMFs with a pseudospherical one). Interestingly, the AMFs calculated for the parallel polarisation are generally larger than those in the perpendicular polarisation, as a consequence of multiple scattering, which affects more the former than
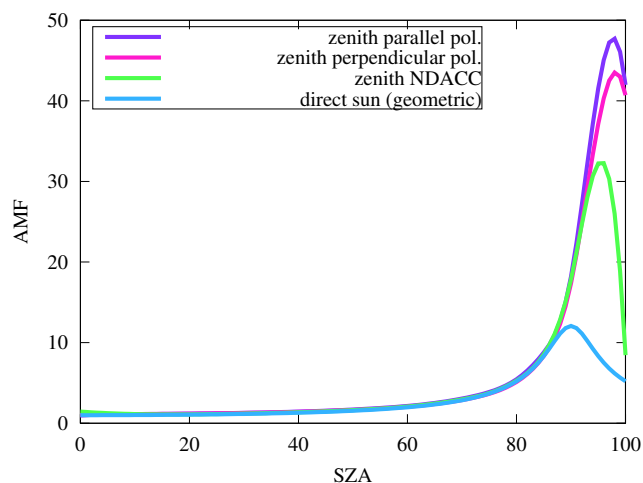
Figure 1. Air mass factors at 430 nm calculated in the zenith direction for both polarisations using the full-spherical SCIATRAN model (Rozanov et al., 2014) and the zenith AMFs suggested by NDACC for the Izaña station as a function of the solar zenith angle. The geometric air mass as used by the standard Brewer algorithm is also depicted for comparison (the NO$_2$ effective height is assumed to be 22 km by the standard algorithm).

the latter. It must be highlighted, on the other hand, that the standard Brewer algorithm incorrectly uses direct sun AMFs for all geometries of observation, which results in overestimations of about 10 % for SZA < 80° and about 60 % at twilight.

4 Calibration campaign

Measurements in direct sun and zenith sky (at two polarisations) observation geometries were continuously taken during daylight hours for a total of 38 days, among which only five were discarded due to rain or fog. The Brewer was operated alternately with the grating at the standard (1000) and optimised (1012) position to allow for comparison between the standard and improved algorithms. Since measurements must be performed in different observation geometries and grating positions, the number of samples to average for each measurement were reduced from 100 (default for direct sun) or 140 (zenith sky) to 16 for both geometries to collect as many observations as possible, as required by the Langley technique.

The standard Langley calibration technique can be rigorously applied only in the case when the absorber vertical column is constant for at least half a day. If this condition is met, Eq. (1) can be represented as a straight line when the linear combination (left side of the equation) is plotted as a function of the air mass factor μ. The calibration constant (first term on the right-hand side) is then the intercept of the linear regression of the observations. However, in the present case, the NO$_2$ concentration increases during the day due to

Table 2. Wavelengths and NO$_2$ weighting coefficients used within the old (Kerr, 1989) and new method at the corresponding grating positions (micro-steps 1000 and 1012, respectively).

Slit	Old wavelength (nm)	Old γ_i	New wavelength (nm)	New γ_i
1	425.104	0	425.236	0.033
2	431.455	0.10	431.586	0.176
3	437.413	−0.59	437.542	−0.510
4	442.893	0.11	443.021	−0.044
5	448.150	1.2	448.276	0.741
6	453.272	−0.82	453.397	−0.396

N$_2$O$_5$ photolysis (Evans et al., 1976) and the Langley technique cannot be applied in its standard formulation. To overcome the issue, many authors (e.g. Roscoe et al., 2001) modified the method by introducing photochemistry-corrected air mass factors. In order to avoid using complex photochemical models, we generalised the Langley technique to include a linear drift of the absorber with time. Indeed, previous studies at the same measurement station (Gil et al., 2008) have already confirmed that the NO$_2$ column linearly increases with time during the day for solar zenith angles below about 80°. Therefore, Eq. (1) was rewritten by explicitly taking into account the dependence on time, t:

$$\sum_i \gamma_i \log I_i = \sum_i \gamma_i \log I_{0_i} \qquad (3)$$
$$- \mu_{NO_2}(t)\, X_{NO_2}(t) \sum_i \gamma_i \sigma_{NO_2 i}.$$

Assuming that, for a given day,

$$X_{NO_2}(t) = \eta(t - t_0) + \xi, \qquad (4)$$

where η is the NO$_2$ daytime increasing rate and ξ the NO$_2$ VCD at time t_0, the solution is easily provided by inverting an over-constrained system, e.g. by calculating a pseudoinverse matrix. The average increasing rate retrieved through the inversion is $(8.2 \pm 1.2) \times 10^{13}$ molecules cm^{-2} h^{-1} and agrees with previous literature (e.g. Sussmann et al., 2005; Gil et al., 2008; Peters et al., 2012), thus proving the effectiveness of the method. As an example, Fig. 2 shows the daily NO$_2$ evolution of direct sun measurements at Izaña on a selected day (269).

The calibration constants for each geometry were calculated from the data gathered at AMFs between 1.5 and 3.5 (direct sun) or 5 (zenith sky). Lower AMFs are not considered because the rate of change of the air mass and the NO$_2$ absorption are small, and changing atmospheric conditions could remarkably affect the regression (Harrison and Michalsky, 1994). Higher AMFs are avoided due to possible shadows from the quartz window border in the field of view (direct sun) and steep variations of NO$_2$ owing to photochemistry.
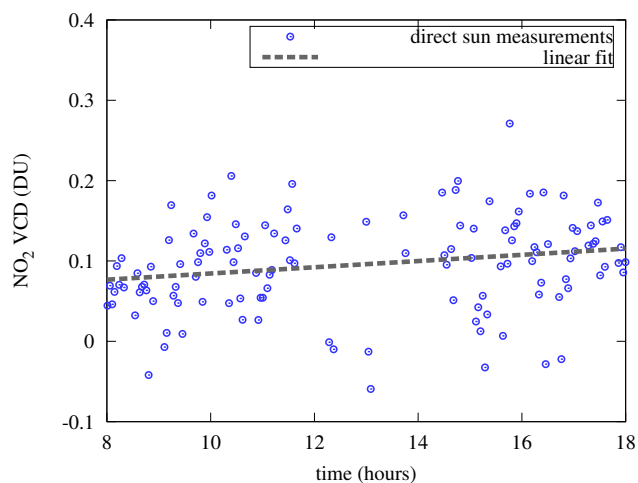
Figure 2. Direct sun VCD measurements at Izaña on day 269 together with a first-order regression line. Despite the high measurement noise, a slight daily evolution can be identified and is about 10^{14} molecules $cm^{-2} h^{-1}$ on the selected day.

5 Results

Estimates of NO₂ column densities using the new algorithm will be described in this section and compared to nearly simultaneous ($\Delta t = 10$ min) data obtained with co-located reference instrumentation associated with NDACC. The comparisons are performed under the optimal conditions of each instrument: direct sun measurements from the Brewer will be examined with reference to those provided by the FTIR, while zenith sky estimates at twilight from the Brewer will be compared to the RASAS retrievals.

5.1 Direct sun measurements

A subset of the data series recorded in the direct sun geometry during the Izaña campaign is displayed, as an example, in Fig. 3. The results with the new algorithm are representative of stratospheric values of 0.1 DU typically reported in the literature (e.g. Brühl and Crutzen, 1993; Gil et al., 2008; Herman et al., 2009), as expected from the clean site of Izaña. Furthermore, although the signal from the Brewer is very noisy, the estimates with the new algorithm also agree with the FTIR data on average. The mean bias between the two sets is −0.012 DU (the Brewer slightly underestimating), which is far below the Brewer uncertainty (Sect. 6), and the root mean square difference is 0.06 DU. Figure 4 displays a histogram of the differences between the two instruments together with an equivalent normal probability distribution function. Normality is verified through the Kolmogorov–Smirnov test (p value = 0.92, calculated under the null hypothesis that the samples are drawn from a normal distribution). The Brewer exhibits some negative VCDs, mostly due to random measurement noise and, to a minor extent, to thin clouds which were not filtered by the cloud-screening
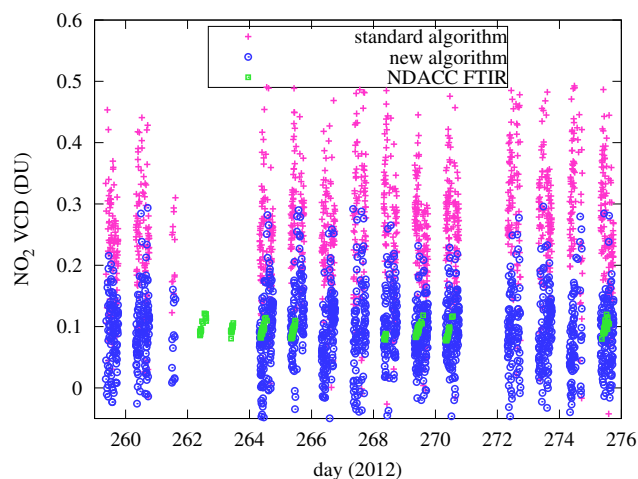

Figure 3. A subset of the NO₂ vertical column densities (VCDs) retrieved in the direct sun geometry during the Izaña calibration campaign. The Brewer data obtained with the grating at the standard position were analysed with the standard algorithm, while the data at the optimised grating position were processed with the new method. FTIR measurements are represented as green squares.
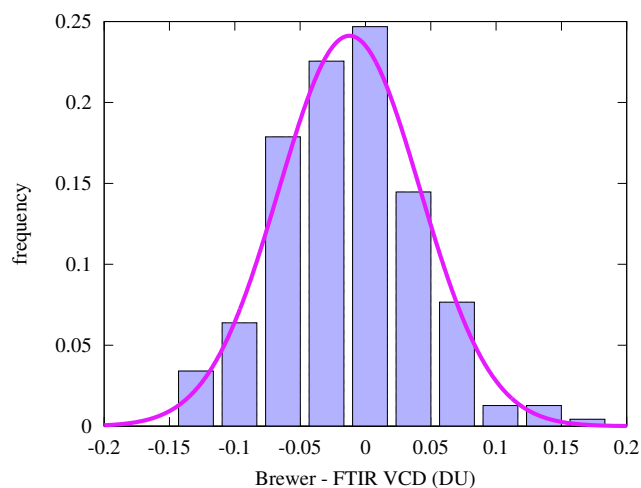
Figure 4. Histogram of the differences between the Brewer and the FTIR estimates in the direct sun geometry. The line represents a normal distribution with same mean (−0.01 DU) and standard deviation (0.05 DU) as the sample distribution.

algorithm. The good comparison with the FTIR on average proves that the negative retrievals are counterbalanced by high positive random errors and the overall bias remains low.

Measurements from the Brewer at the standard set of wavelengths have been processed as well with the standard algorithm (after calculating the corresponding extraterrestrial constant). The retrieval by the standard algorithm remarkably overestimates, with values about 100 % higher than the new algorithm. These differences are in good agreement with previous model studies (Diémoz et al., 2013).
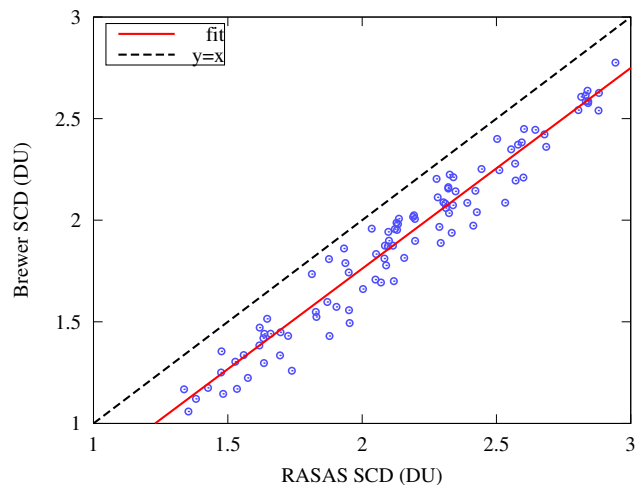
Figure 5. Scatterplot between twilight SCDs by the Brewer (zenith sky, perpendicular polarisation) and the reference RASAS-II spectrometer. Intercept: -0.2 DU; slope: 0.99; R^2: 0.95.

Figure 6. Same as in Fig. 5, with the Brewer operating in parallel polarisation. Intercept: 0.7 DU; slope: 0.85; R^2: 0.76.

5.2 Zenith sky measurements

Figure 5 shows the scatterplot between the estimates by the Brewer operating in the perpendicular polarisation and the RASAS-II spectrometer. This zenith sky comparison is performed in terms of slant column densities (SCDs) to overcome any issues related to different zenith sky AMF calculations between algorithms. Also, both instruments use the same spectroscopic data sets and effective temperatures to retrieve NO$_2$. Although correlation between the two series is evident (Pearson's correlation coefficient $\rho = 0.98$; $R^2 = 0.95$; slope $= 0.99$), a nearly constant offset of -0.2 DU (distance between the regression line and the $y = x$ line) can be observed between the series. This underestimation by the Brewer, corresponding to a mean bias in the vertical column of -0.015 DU over the measured range, is slightly lower than the estimated uncertainty of the Brewer for zenith sky measurements (Sect. 6.3).

The comparison between RASAS-II retrievals and zenith sky measurements in parallel polarisation by the Brewer is shown in Fig. 6. This time, both the correlation ($\rho = 0.87$; $R^2 = 0.76$) and the fit parameters (slope $= 0.85$; intercept $= 0.7$ DU) are worse compared to the perpendicular polarisation. The corresponding mean bias in the vertical column is 0.013 DU over the measurement range.

In principle, the discrepancies between the two instruments could be due to inaccuracies in determining the Brewer ETCs in both polarisations (notably, the constant offset in the perpendicular polarisation data set). However, no better results throughout the full range of AMFs were found by perturbing the values of the calibration constants, which degrades the comparison at either low or high AMFs (not shown). The results of the comparison certainly show the need for further investigation and work, e.g. a longer
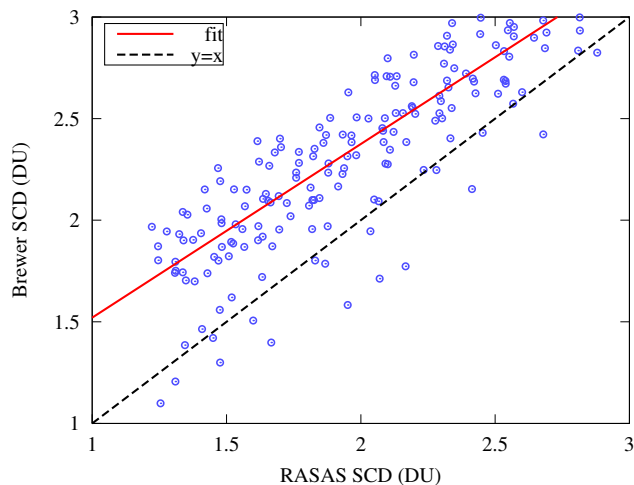
intercomparison campaign. However, one of the likely reasons may be already found in the Ring effect, which would explain the slightly larger effect on parallel polarisation compared to the perpendicular one, as found by Barton (2007). More details are provided in Sect. 6.3.

Finally, it must be noted that the root mean square (rms) residual of the fit between the two data sets (0.96 DU for SCDs in perpendicular polarisation and 3.3 DU for parallel polarisation) can be further decreased by averaging a larger number of the samples for each measurement.

6 Uncertainty budget

The uncertainty estimate in Brewer measurements is a complex task owing to the large number of the involved parameters and their reciprocal correlations. Furthermore, an analytic assessment of the uncertainty is not feasible and the influence of the various factors on the retrieved NO$_2$ is expected to be non-linear. A Monte Carlo method (MCM) approach (BIPM et al., 2008) was therefore adopted.

In this section, the Brewer uncertainty will be discussed for three different cases. In the first scenario, the relatively simple case of direct sun measurements in a pristine site with similar characteristics as the Izaña observatory will be discussed. In the second simulation, the Brewer is assumed to be initially calibrated at a pristine site, as in case 1, but then moved to a more polluted environment for operation. Finally, in the third part, the uncertainty of zenith sky measurements will be discussed for the same environmental conditions as in case 1. It must be noted that case 1 and 3 must be analysed independently, since the uncertainty of not only the AMFs but also of slant column densities may potentially differ between both geometries, e.g. due to the different light intensity and filters used.

6.1 Case 1: direct sun measurements at a pristine site

The first scenario assumes that the Brewer operates at the same high-altitude site (only stratospheric NO$_2$ is considered, with VCD $= 0.1$ DU) where the Langley plot has been performed and that the atmospheric conditions remain constant compared to the calibration period. Several sources of uncertainties, both in the calibration and the measurement phase, are considered taking into account the instrumental characteristics of Brewer #066:

1. Random noise was artificially added to the measured count rates during both the Langley calibration and the measurements, using samples from a Poisson distribution centred at the measured number of photons, and scaled corresponding to the number of samples recorded at each measurement.

2. The standard deviation of the spectral attenuations of the neutral density filters measured during the diagnostic internal tests was used to assess the uncertainty in the filter correction. Additionally, the measurements were randomly perturbed by simulating the effect of thin clouds successfully passing the cloud-screening algorithm and the filters were then simulated to switch as a function of the intensity of the solar light.

3. An uncertainty in the operational wavelengths of 0.02 nm was assumed based on some tests and previous literature (e.g. Kerr and Davis, 2007).

4. The dead time was assumed to be determined within an uncertainty of 10 %.

5. Diffuse light in the field of view of the instrument was assessed to be negligible in the visible range and for the Izaña conditions, according to radiative transfer calculations.

6. Stray light in the monochromator was not considered in the study. It is however assumed to be negligible for visible wavelengths. This is in large part due to the fact that in the visible spectrum, the intensity levels across slits are more even compared to the UV (with several orders of magnitude from slit 1 to 5), therefore the relative change in intensity will be small and about the same on all slits.

7. The uncertainties of the ozone and nitrogen dioxide laboratory cross sections were assumed to be 3 and 4 %, respectively, based on previous literature (see references in Table 1).

8. The effect of the aerosol Ångström exponent, representative of the spectral curvature of the aerosol optical depth, was assessed by varying its value between 0.2 and 1.6, based on the Aerosol Robotic Network (AERONET) data gathered at Izaña in October 2012.

9. A conservative uncertainty of 10 % was assumed for the measured resolution at each slit.

10. 20 K and 5 km were taken as the uncertainties of the NO$_2$ effective temperature and height, respectively (Redondas and Cede, 2007). The NO$_2$ profile is expected to not remarkably impact the direct sun AMF, which is calculated as the secant of the SZA at the mean height of the absorber layer (assumed to be 27 km). This approximation is considered to be accurate for SZAs $< 80°$.

11. An uncertainty of 30 % was assumed for the O$_2$−O$_2$ correction in the retrieval.

A large number (1000) of samples from the probability density functions (PDFs) of the above-mentioned factors were employed, and the NO$_2$ retrieval was simulated at each iteration with a different set of variables. The standard deviation of all NO$_2$ retrievals was then taken as the standard (combined) uncertainty of the measurement as a function of the solar zenith angle. The latter was varied within the same range of measurement as in the campaign (78° being the maximum SZA due to shadows by the quartz window border in the direct sun field of view). Figure 7 shows that the VCD uncertainty ranges from 0.05 to 0.19 DU with smaller values for large SZAs (due to the larger NO$_2$ absorption). It is worth noting that the standard uncertainty can be approximately as high as twice the value of the measurements made in Izaña. The two largest contributions to the uncertainty are linked to the wavelength uncertainty, discussed in more depth in Sect. 7.1, and Poisson noise. The latter can be further reduced by increasing the number of samples (which were decreased for the Langley plot, as described in Sect. 4). Finally, the influence of the filter uncertainty on direct sun measurements is generally low, since Brewer #066 employs only few and weak density filters in this observation geometry at the Izaña conditions.

6.2 Case 2: direct sun measurements at a polluted site

The second case is representative of a Brewer spectrophotometer accurately calibrated at a high-altitude site without tropospheric NO$_2$ (VCD $= 0.1$ DU) and then operated at a polluted site. The calibration was simulated with the same criteria as in case 1. Conversely, the measurement phase presents some relevant differences:

1. The standard atmosphere (Anderson et al., 1986) was modified by including a 5 km thick polluted layer above ground (NO$_2$ concentration 4×10^{10} mol cm^{-2}), thus increasing to 1 DU the total nitrogen dioxide VCD.

2. The NO$_2$ effective height used in the calculations was decreased to 10 km (the actual height is not influential for direct sun retrievals) with an uncertainty of 5 km.

3. The NO$_2$ effective temperature was increased to 260 K and the corresponding uncertainty was set to 20 K.
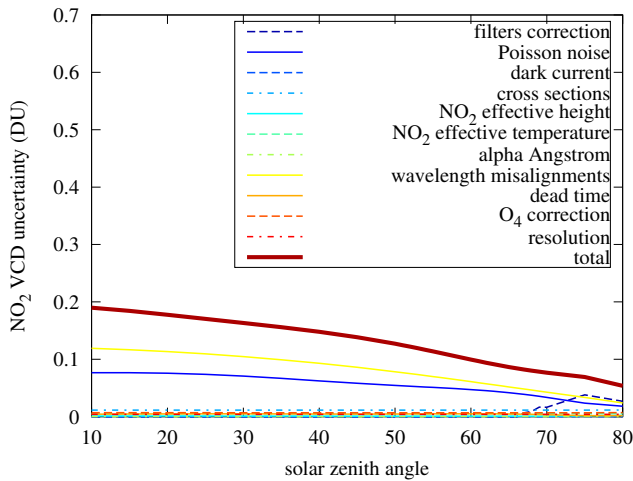
Figure 7. Monte Carlo standard uncertainty for Brewer NO$_2$ measurements in direct sun geometry in Izaña (NO$_2$ VCD set to 0.1 DU).

Figure 8. Monte Carlo standard uncertainty for Brewer NO$_2$ measurements in direct sun geometry at a polluted site (NO$_2$ VCD assumed to be 0.1 DU during the calibration phase and 1 DU during measurements).
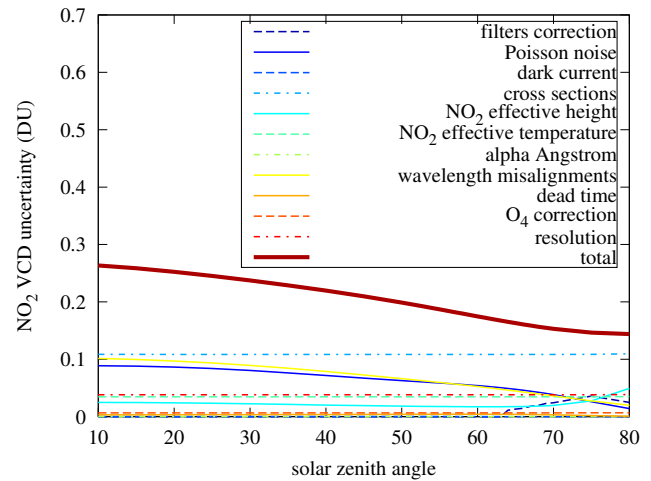
4. The altitude and pressure of the measurement site were set to 570 m a.s.l. and 950 hPa, respectively, i.e. the conditions of the original location of Brewer #066 in Aosta, Italy. The O$_2$−O$_2$ correction was updated correspondingly.

Figure 8 shows the uncertainty estimated for case 2. Compared to case 1, the overall absolute uncertainty increases (0.14–0.27 DU, depending on the SZA), but the relative uncertainty, i.e. the ratio between total uncertainty and the NO$_2$ VCD, remarkably decreases (to 14–26 %), revealing that the quality of Brewer estimates in direct sun geometry is higher for larger NO$_2$ columns. Moreover, it must be noted that the contribution of the cross-section uncertainty to the overall uncertainty increases for case 2 compared to case 1, as also expected from the propagation of uncertainty in Eq. (1) (the cross section uncertainty being proportional to the total NO$_2$ content in the atmosphere). Finally, it is important to mention that if the Brewer were calibrated at a polluted site, the main assumption of the constant atmospheric conditions needed by the Langley technique would not be met. This case is beyond the scope of the paper and will not be discussed here.

6.3 Case 3: zenith sky measurements at a pristine site

In the last scenario, zenith sky measurements are simulated in the same conditions as in case 1 (VCD = 0.1 DU). In this third case, however,

1. the measured irradiances are different from case 1, as is their dependence on the SZA, due to the different observation geometry and set of filters used. Indeed, in direct sun measurements, a thick filter is placed before the other neutral density filters, whereas a thinner polarising filter is used for the zenith sky geometry;

2. the zenith sky AMFs are much more impacted by the atmospheric profiles than the direct sun AMFs. A sensitivity study was performed using several atmospheric profiles and aerosol loads. The resulting AMF uncertainty ranges from about 2 % at SZA = 60° to 8 % at SZA = 20°. At twilight, the AMF uncertainty is 7 %, in accordance with the results by Gil et al. (2008).

The zenith sky uncertainty is depicted in Figs. 9 and 10 for the parallel and perpendicular polarisations, respectively. A notable contribution is given by the filter uncertainty. Indeed, thicker filters, which are characterised by higher uncertainty, are used at low SZAs for zenith sky estimates. This impacts not only measurements, but also the calibration.

The analysis, however, does not take into account some likely major contributors to the zenith sky uncertainty, which are difficult to quantify. First, diffuse irradiance is impacted by the Ring effect, which even state-of-the-art radiative transfer models cannot accurately reproduce at present by taking polarisation into account at the same time. A previous study by Barton (2007) reported considerable overestimations by the Brewer (up to 800 %) due to the Ring effect, especially using parallel polarisation, but the author himself admits that those results could have been compromised by unrealistic simulations by the radiative transfer model used. In the present work, simulations of unpolarised zenith sky irradiances with and without taking into account rotational Raman scattering (RRS) gave rise to VCD differences of 0.02–0.06 DU, with a marked SZA dependence. However, the effect using polarised irradiances could be different.

A second contributing factor to the uncertainty of zenith sky estimates is the unknown efficiency of the polarising filter, likely lower than 100 %. As a consequence, photons from the zenith polarisation could be detected by the Brewer even
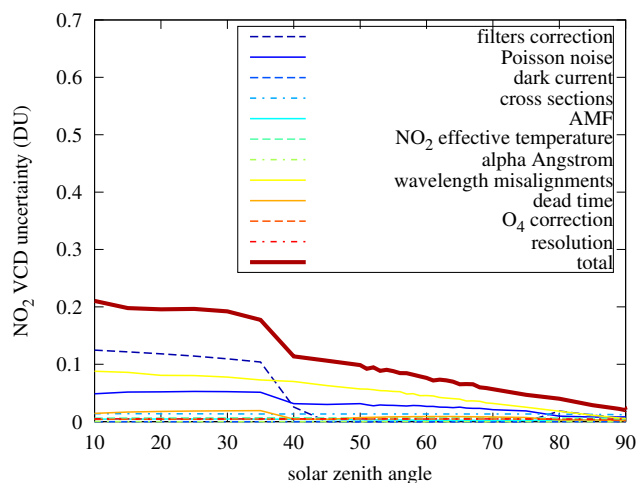
Figure 9. Monte Carlo standard uncertainty for Brewer NO$_2$ measurements in the zenith sky geometry and parallel polarisation in Izaña (NO$_2$ VCD set to 0.1 DU).

Figure 10. Monte Carlo standard uncertainty for Brewer NO$_2$ measurements in the zenith sky geometry and perpendicular polarisation in Izaña (NO$_2$ VCD set to 0.1 DU).
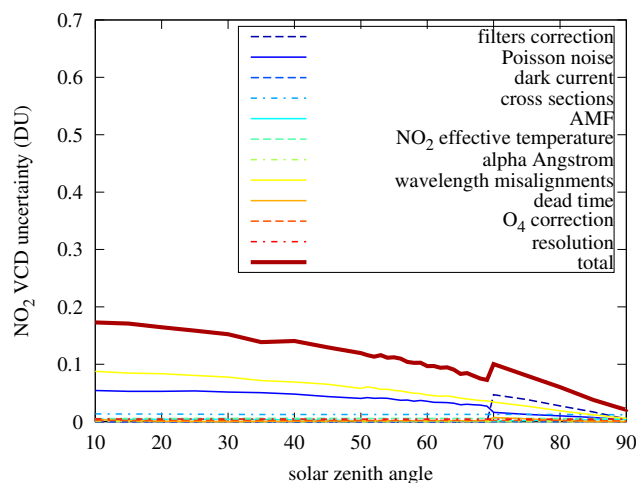
when the instrument is supposed to measure in the parallel plane (more light is expected from the perpendicular polarisation at twilight), thus representing a relevant source of stray light. Both issues should be investigated in more detail in future work.

Finally, it should be kept in mind that when zenith sky SCDs by the Brewer and RASAS are compared, one should not take into account the uncertainty contribution from the AMFs (only employed for SCD to VCD conversion), cross sections and NO$_2$ effective temperature (since the same set of cross sections is used for both instruments). The resulting SCD uncertainty at twilight decreases then to 0.25 DU for both polarisations.

7 Discussion

7.1 Sensitivity to wavelength

In a Brewer spectrophotometer, the wavelength scale is adjusted with reference to the line emission spectrum of a mercury lamp. The test gives the position of the line (usually, at about 296 or 302 nm) to the precision of about 0.1 steps. Some factors, however, may degrade the instrumental wavelength alignment. Temperature changes inside the monochromator, for example, can affect the positioning to an extent of about 0.3 steps K^{-1}. Also large relocations of the grating, e.g. due to scanning routines or switch of the diffraction order of the grating from ozone to nitrogen dioxide measurements, can slightly misplace the wavelength scale if the micrometer is not working properly. Moreover, the accuracy – and thus, the uncertainty – is additionally determined by errors on the dispersion function and changes to the optical axes, including lamp reference alignments and intensity of the lamp (relative intensity of multiplet lines).

The uncertainty analysis in the present paper clearly proves that an optimal choice of the grating position is not sufficient to remove the Brewer sensitivity to wavelength misalignments and to reach the required accuracy. Indeed, the wavelength uncertainty remains a major contributor to the overall measurement uncertainty and more efforts must be spent in the future to solve the issue. As a step forward, an alternative and possibly more effective approach consists of including the wavelength shift in the algorithm, such as in Kerr (2002) and Cede et al. (2006). One degree of freedom can be reserved to an additional vector, the wavelength derivative of the solar spectrum. The obtained vector would not only absorb any small wavelength misalignment, thus improving the stability of the retrieval, but it would also provide an indication of the wavelength accuracy of the instrument. This would be an essential quality parameter in the reprocessing of historical data sets.

7.2 Reprocessing of historical data sets

Every Brewer stores all raw data in its files (B-files). Moreover, the standard routines already measure the solar irradiance through all six slits, although data at only five wavelengths are traditionally processed by the retrieval algorithm. This makes it possible, in principle, to apply the new algorithm to past time series. However, some fundamental steps are required prior to reprocessing historical data sets:

1. In order to recalculate the specific set of weighting factors for each instrument, the dispersion function must be well characterised. To this purpose, the traditional Brewer dispersion test, based on the identification of several emission lines (e.g. from mercury, cadmium or zinc lamps), has been updated to reprocess the lines in the visible range and is now accessible to the entire

Brewer user community as a software update. As an alternative, the diffraction grating law can be applied to calculate the dispersion function in the visible from the dispersion in the UV (normally measured during ozone calibration campaigns). Although the grating position at which the historical series has been measured may not be optimal for a specific instrument, the new algorithm can still be applied to the standard wavelengths used for the retrieval. Additionally, it provides an estimate of the uncertainty due to non-optimised settings. Furthermore, tests using a unique set of weightings for several Brewers are currently being performed to assess the sensitivity to different dispersion functions and wavelength settings.

2. The spectral attenuation of the filters must be well known, especially when using high attenuation filters. Based on a preliminary analysis, each single instrument manifests different properties and must be independently characterised. A new routine has been developed to assess the spectral attenuation of each filter in the visible range using the internal lamp. However, since noise is considerable when using the thickest filters, a great number of tests should be scheduled. An alternative approach is to statistically analyse the long-term series and retrieve the effect of filters by forcing the continuity of the NO$_2$ retrievals between contiguous measurements with different filters.

3. The ETC should be determined. If a Langley campaign at a high-altitude site or calibration transfer from a travelling standard are not feasible, statistical methods such as the minimum-amount Langley extrapolation or the bootstrap method (e.g. Cede et al., 2006; Herman et al., 2009) are available to provide the necessary extraterrestrial calibration constant. Unfortunately, in all cases, calibration drifts can occur after some time. To investigate the Brewer stability, the following techniques are suggested: measurements obtained with the internal standard lamp as a source, instead of the sun, may be used to track the ETC (standard lamp test); statistical techniques to determine the ETC could be applied on several time portions of the series and the results could be compared; the analysis of the wavelength shifts, relative to the Fraunhofer solar structure (Slaper et al., 1995), in the UV spectra measured by a Brewer could provide very valuable information about any wavelength instabilities affecting the retrieval. Also, a detailed logbook of the instrument, constantly updated by the operator, is essential to keep track of any maintenance or replacements. In the event that some discontinuities are identified, a piecewise calibration may be applied to different portions of the series.

7.3 Updates to the Brewer operational software

Once the performances of the new algorithm have been extensively studied, the Brewer operational software may be updated with little effort and shared with the Brewer user community. This will let all research groups benefit from the improvements, even those without any radiative calculation experience. The weighting coefficients, which are hard-coded into the software at present, should instead be read from an external file, which can differ among instruments and be provided by calibration facilities or other research groups. The same modification should be applied to take into account the spectral sensitivity of the attenuation filters, as the software already does when calculating the aerosol optical depth. As for the grating position and the differential cross section, the Brewer software already allows for adjusting their values in the configuration files. Unpolarised zenith sky AMFs can be easily calculated using the software provided by NDACC (Van Roozendael and Hendrick, 2012) for the selected measuring site and stored in an external file, which the Brewer software should be instructed to read from. The error on AMF resulting from neglecting the polarisation was found to be low at twilight (last point of Sect. 3). Finally, the oxygen dimer interference was found to be unimportant and may be neglected to a first approximation.

8 Conclusions

A new algorithm to retrieve the nitrogen dioxide by MKIV Brewers was tested using data recorded during a calibration campaign at a high-altitude site. An extension of the Langley technique, suitable for very clean sites without tropospheric NO$_2$ and taking into account the daytime increase of the NO$_2$ column, was developed to overcome issues related to the diurnal change in the absorber and was found to provide results in agreement with the previous literature. The retrieval with the new algorithm no longer shows the overestimations which affect the standard method, which can be as large as 100 %, and is less influenced by the interference from other species and instrumental factors. Comparisons of the Brewer measurements to two reference NDACC radiometers were performed, with generally good correlations and mean biases in the vertical column amounts of −0.012, −0.015, and 0.013 DU for direct sun and twilight zenith sky, the latter at perpendicular and parallel polarisations, respectively, over the corresponding measurement ranges. Furthermore, the assessment of the uncertainty of Brewer measurements was performed using the Monte Carlo technique. Although the Ring effect could represent a major source of uncertainty, its contribution to polarised light is tricky to quantify at present and was not taken into account in the MCM budget. Further work is needed on this issue. Although the combined uncertainty can be further reduced by increasing the number of samples for each measurement (thus decreasing the Pois-

son noise), a large contribution persists which is due to the uncertainty of the operating wavelengths. A possible solution including the derivative of the solar spectrum in the retrieval was presented and additional efforts will be made in that regard. Finally, the method was tested in a very clean environment, with a NO$_2$ contribution mostly from the stratosphere; however, the relative uncertainty of the direct sun measurements is expected to decrease in more polluted conditions, thus making the Brewer a good instrument to monitor nitrogen dioxide, for example, in large cities. It is therefore recommended to schedule nitrogen dioxide measurements on all existing MKIV Brewers. Partitioning between the stratospheric and the tropospheric NO$_2$ content, making use of nearly simultaneous direct sun and zenith sky estimates by the Brewer, will be addressed in future work.

Since every Brewer stores all raw data (at all six slits) in its files, the method can be applied to reprocess past time series as well. A new set of weightings can be easily calculated for different Brewer instruments provided that the dispersion is well characterised. Additionally, statistical calibration methods are available to provide the necessary extraterrestrial constant when a Langley campaign is not feasible.

Edited by: L. Lamsal

References

Aliwell, S. R., Van Roozendael, M., Johnston, P. V., Richter, A., Wagner, T., Arlander, D. W., Burrows, J. P., Fish, D. J., Jones, R. L., Tørnkvist, K. K., Lambert, J.-C., Pfeilsticker, K., and Pundt, I.: Analysis for BrO in zenith-sky spectra: an intercomparison exercise for analysis improvement, J. Geophys. Res., 107, ACH10.1–ACH10.20, doi:10.1029/2001JD000329, 2002.

Anderson, G. P., Clough, S., Kneizys, F., Chetwynd, J., and Shettle, E. P.: AFGL atmospheric constituent profiles (0.120 km), DTIC Document, Tech. rep., 1986.

Barton, D. V.: The measurement of NO$_2$ using Brewer spectrophotometers, M.S. thesis, York University, Toronto, Ontario, 2007.

BIPM, IEC, IFCC, ILAC, ISO, and IUPAC: Evaluation of Measurement Data – Supplement 1 to the Guide to the Expression of Uncertainty in Measurement – Propagation of distributions using a Monte Carlo method, Joint Committee for Guides in Metrology, Joint Committee for Guides in Metrology, 101, 2008.

Bodhaine, B. A., Wood, N. B., Dutton, E. G., and Slusser, J. R.: On Rayleigh optical depth calculations, J. Atmos. Ocean. Tech., 16, 1854–1861, doi:10.1175/1520-0426(1999)016<1854:ORODC>2.0.CO;2, 1999.

Bogumil, K., Orphal, J., Homann, T., Voigt, S., Spietz, P., Fleischmann, O. C., Vogel, A., Hartmann, M., Kromminga, H.,

Bovensmann, H., Frerick, J., and Burrows, J. P.: Measurements of molecular absorption spectra with the SCIAMACHY preflight model: instrument characterization and reference data for atmospheric remote-sensing in the 230–2380 nm region, J. Photoch. Photobio. A, 157, 167–184, doi:10.1016/S1010-6030(03)00062-5, 2003.

Bouguer, P.: Essai d'optique sur la gradation de la lumière, edited by: Jombert, C., Paris, 1729.

Brewer, A. W. and McElroy, C. T.: Nitrogen dioxide concentrations in the atmosphere, Nature, 246, 129–133, doi:10.1038/246129a0, 1973.

Brühl, C. and Crutzen, P. J.: MPIC two-dimensional model, NASA Ref. Publ., 1292, 103–104, 1993.

Cede, A., Herman, J., Richter, A., Krotkov, N., and Burrows, J.: Measurements of nitrogen dioxide total column amounts using a Brewer double spectrophotometer in direct sun mode, J. Geophys. Res., 111, D05304, doi:10.1029/2005JD006585, 2006.

Crutzen, P. J.: The influence of nitrogen oxides on the atmospheric ozone content, Q. J. Roy. Meteor. Soc., 96, 320–325, doi:10.1002/qj.49709640815, 1970.

Diémoz, H., Tarricone, C., Agnesod, G., Siani, A. M., and Casale, G. R.: Brewer #066: a new location in Italy, in: The Tenth Biennial WMO Consultation on Brewer Ozone and UV Spectrophotometer Operation, Calibration and Data Reporting, edited by: McElroy, C. T. and Hare, E. W., Gaw Report, 32–33, 2007.

Diémoz, H., Savastiouk, V., and Siani, A. M.: Capability and limitations in measuring atmospheric nitrogen dioxide column amounts by means of the MKIV Brewer spectrophotometers, Vol. 8890, doi:10.1117/12.2028704, 2013.

Evans, W., Kerr, J., Wardle, D., McConnell, J., Ridley, B., and Schiff, H.: Intercomparison of NO, NO$_2$ and HNO$_3$ measurements with photochemical theory, Atmosphere, 14, 189–198, doi:10.1080/00046973.1976.9648415, 1976.

Francesconi, M., Casale, G., Siani, A., and Casadio, S.: Ground-based NO$_2$ measurements at the Italian Brewer stations: a pilot study with Global Ozone Monitoring Experiment (GOME), Nuovo Cimento C, 27, 383–392, doi:10.1393/ncc/i2004-10036-8, 2004.

Gil, M., Yela, M., Gunn, L. N., Richter, A., Alonso, I., Chipperfield, M. P., Cuevas, E., Iglesias, J., Navarro, M., Puentedura, O., and Rodríguez, S.: NO$_2$ climatology in the northern subtropical region: diurnal, seasonal and interannual variability, Atmos. Chem. Phys., 8, 1635–1648, doi:10.5194/acp-8-1635-2008, 2008.

Grainger, J. and Ring, J.: Anomalous Fraunhofer line profiles, Nature, 193, 762, doi:10.1038/193762a0, 1962.

Gröbner, J., Wardle, D. I., McElroy, C. T., and Kerr, J. B.: Investigation of the wavelength accuracy of Brewer spectrophotometers, Appl. Optics, 37, 8352–8360, doi:10.1364/AO.37.008352, 1998.

Haagen-Smit, A. J.: Chemistry and physiology of Los Angeles smog, Ind. Eng. Chem., 44, 1342–1346, doi:10.1021/ie50510a045, 1952.

Hampson, J.: Photochemical Behaviour of the Ozone Layer, Canadian Armament Research and Development Establishment, 1964.

Harrison, L. and Michalsky, J.: Objective algorithms for the retrieval of optical depths from ground-based measurements, Appl. Optics, 33, 5126–5132, doi:10.1364/AO.33.005126, 1994.

Herman, J., Cede, A., Spinei, E., Mount, G., Tzortziou, M., and Abuhassan, N.: NO$_2$ column amounts from ground-

based Pandora and MFDOAS spectrometers using the direct-sun DOAS technique: Intercomparisons and application to OMI validation, J. Geophys. Res., 114, D13307, doi:10.1029/2009JD011848, 2009.

Hermans, C., Vandaele, A., Fally, S., Carleer, M., Colin, R., Coquart, B., Jenouvrier, A., and Merienne, M.-F.: Absorption cross-section of the collision-induced bands of oxygen from the UV to the NIR, in: Weakly Interacting Molecular Pairs: Unconventional Absorbers of Radiation in the Atmosphere, Springer, 193–202, 2003.

Hofmann, D., Bonasoni, P., De Maziere, M., Evangelisti, F., Giovanelli, G., Goldman, A., Goutail, F., Harder, J., Jakoubek, R., Johnston, P., Kerr, J., Matthews, W. A., McElroy, T., McKenzie, R., Mount, G., Platt, U., Pommereau, J.-P., Sarkissian, A., Simon, P., Solomon, S., Stutz, J., Thomas, A., Van Roozendael, M., and Wu, E.: Intercomparison of UV/visible spectrometers for measurements of stratospheric NO$_2$ for the Network for the Detection of Stratospheric Change, J. Geophys. Res., 100, 16765–16791, doi:10.1029/95JD00620, 1995.

Johnston, H. S. and Graham, P.: Unpublished Absorption Coefficients on NO$_2$ and O$_3$, Dept. of Chem., University of California, Berkeley, 1976.

Jones, R. L., Austin, J., McKenna, D. S., Anderson, J. G., Fahey, D. W., Farmer, C. B., Heidt, L. E., Kelly, K. K., Murphy, D. M., Proffitt, M. H., Tuck, A. F., and Vedder, J. F.: Lagrangian photochemical modeling studies of the 1987 Antarctic spring vortex: 1. Comparison with AAOE observations, J. Geophys. Res., 94, 11529–11558, doi:10.1029/JD094iD09p11529, 1989.

Kerr, J.: Ground-based measurements of nitrogen dioxide using the Brewer spectrophotometer, in: Ozone in the Atmosphere, Vol. 1, 340 pp., 1989.

Kerr, J. B.: New methodology for deriving total ozone and other atmospheric variables from Brewer spectrophotometer direct sun spectra, J. Geophys. Res., 107, 4731, doi:10.1029/2001JD001227, 2002.

Kerr, J. B. and Davis, J. M.: New methodology applied to deriving total ozone and other atmospheric variables from global irradiance spectra, J. Geophys. Res., 112, D21301, doi:10.1029/2007JD008708, 2007.

Kipp and Zonen: MKIV Brewer Spectrophotometer – Instruction Manual, Delft, 2007.

Kumharn, W., Rimmer, J. S., Smedley, A. R., Ying, T. Y., and Webb, A. R.: Aerosol optical depth and the global brewer network: a study using UK-and Malaysia-based Brewer spectrophotometers, J. Atmos. Ocean. Tech., 29, 857–866, doi:10.1175/JTECH-D-11-00029.1, 2012.

McElroy, C., Elokhov, A., Elansky, N., Frank, H., Johnston, P., and Kerr, J.: Visible light nitrogen dioxide spectrophotometer intercomparison: Mount Kobau, British Columbia, 28 July to 10 August, 1991, NASA, Goddard Space Flight Center, Ozone in the Troposphere and Stratosphere, Part 2, 663–666 (SEE N 95-11006 01-47), 1994.

Peters, E., Wittrock, F., Großmann, K., Frieß, U., Richter, A., and Burrows, J. P.: Formaldehyde and nitrogen dioxide over the remote western Pacific Ocean: SCIAMACHY and GOME-2 validation using ship-based MAX-DOAS observations, Atmos. Chem. Phys., 12, 11179–11197, doi:10.5194/acp-12-11179-2012, 2012.

Puentedura, O., Gil, M., Saiz-Lopez, A., Hay, T., Navarro-Comas, M., Gómez-Pelaez, A., Cuevas, E., Iglesias, J., and Gomez, L.: Iodine monoxide in the north subtropical free troposphere, Atmos. Chem. Phys., 12, 4909–4921, doi:10.5194/acp-12-4909-2012, 2012.

Redondas, A. and Cede, A.: Brewer algorithm sensitivity analysis, in: The Tenth Biennial WMO Consultation on Brewer Ozone and UV Spectrophotometer Operation, Calibration and Data Reporting, edited by: McElroy, C. T. and Hare, E. W., Gaw Report, 12–14, 2007.

Roscoe, H., Charlton, A., Fish, D., and Hill, J.: Improvements to the accuracy of measurements of NO$_2$ by zenith-sky visible spectrometers II: errors in zero using a more complete chemical model, J. Quant. Spectrosc. Ra., 68, 337–349, doi:10.1016/S0022-4073(00)00058-3, 2001.

Rothman, L. S., Gordon, I. E., Barbe, A., Chris Benner, D., Bernath, P. F., Birk, M., Boudon, V., Brown, L. R., Campargue, A., Champion, J.-P., Chance, K., Coudert, L. H., Dana, V., Devi, V. M., Fally, S., Flaud, J.-M., Gamache, R. R., Goldman, A., Jacquemart, D., Kleiner, I., Lacome, N., Lafferty, W. J., Mandin, J.-Y., Massie, S. T., Mikhailenko, S. N., Miller, C. E., Moazzen-Ahmadi, N., Naumenko, O. V., Nikitin, A. V., Orphal, J., Perevalov, V. I., Perrin, A., Predoi-Cross, A., Rinsland, C. P., Rotger, M., Šimečková, M., Smith, M. A. H., Sung, K., Tashkun, S. A., Tennyson, J., Toth, R. A., Vandaele, A. C., and Vander Auwera, J.: The HITRAN 2008 molecular spectroscopic database, J. Quant. Spectrosc. Ra., 110, 533–572, doi:10.1016/j.jqsrt.2009.02.013, 2009.

Rozanov, V. V. and Rozanov, A. V.: Differential optical absorption spectroscopy (DOAS) and air mass factor concept for a multiply scattering vertically inhomogeneous medium: theoretical consideration, Atmos. Meas. Tech., 3, 751–780, doi:10.5194/amt-3-751-2010, 2010.

Rozanov, V., Rozanov, A., Kokhanovsky, A., and Burrows, J.: Radiative transfer through terrestrial atmosphere and ocean: software package SCIATRAN, J. Quant. Spectrosc. Ra., 133, 13–71, doi:10.1016/j.jqsrt.2013.07.004, 2014.

Schneider, M., Blumenstock, T., Chipperfield, M. P., Hase, F., Kouker, W., Reddmann, T., Ruhnke, R., Cuevas, E., and Fischer, H.: Subtropical trace gas profiles determined by ground-based FTIR spectroscopy at Izaña (28° N, 16° W): Five-year record, error analysis, and comparison with 3-D CTMs, Atmos. Chem. Phys., 5, 153–167, doi:10.5194/acp-5-153-2005, 2005.

Slaper, H., Reinen, H. A. J. M., Blumthaler, M., Huber, M., and Kuik, F.: Comparing ground-level spectrally resolved solar UV measurements using various instruments: A technique resolving effects of wavelength shift and slit width, Geophys. Res. Lett., 22, 2721–2724, doi:10.1029/95GL02824, 1995.

Shaw, G. E.: Nitrogen dioxide optical absorption in the visible, J. Geophys. Res., 81, 5791–5792, doi:10.1029/JC081i033p05791, 1976.

Solomon, S., Portmann, R. W., Sanders, R. W., Daniel, J. S., Madsen, W., Bartram, B., and Dutton, E. G.: On the role of nitrogen dioxide in the absorption of solar radiation, J. Geophys. Res., 104, 12047–12058, doi:10.1029/1999JD900035, 1999.

Sussmann, R., Stremme, W., Burrows, J. P., Richter, A., Seiler, W., and Rettinger, M.: Stratospheric and tropospheric NO$_2$ variability on the diurnal and annual scale: a combined retrieval from ENVISAT/SCIAMACHY and solar FTIR at the Permanent

Ground-Truthing Facility Zugspitze/Garmisch, Atmos. Chem. Phys., 5, 2657–2677, doi:10.5194/acp-5-2657-2005, 2005.

Van Roozendael, M. and Hendrick, F.: Recommendiations for NO$_2$ column retrieval from NDACC zenith-sky UV-VIS spectropho-tometers, Tech. rep., Network for the Detection of Atmospheric Composition Change (NDACC), 2012.

Vandaele, A. C., Hermans, C., Fally, S., Carleer, M., Colin, R., Mérienne, M.-F., Jenouvrier, A., and Coquart, B.: High-resolution Fourier transform measurement of the NO$_2$ visi-ble and near-infrared absorption cross sections: temperature and pressure effects, J. Geophys. Res., 107, ACH3.1–ACH3.12, doi:10.1029/2001JD000971, 2002.

Vigroux, E.: Absorption de l'ozone dans le spectre visible, Compt. Rend. Acad. Sci. Paris, 235, 149–150, 1952.